PROCEEDINGS OF SCIENCE

Study of Majorana Fermion Dark Matter

Gwo-Guang Wong*
Department of Physics and Chung Yuan Center for High Energy Physics,
Chung Yuan Christian University,
Chung-Li, Taiwan 320, Republic of China E-mail: ggwong@cycu.edu.tw

Chun-Khiang Chua
Department of Physics and Chung Yuan Center for High Energy Physics,
Chung Yuan Christian University,
Chung-Li, Taiwan 320, Republic of China E-mail: ckchua@cycu.edu.tw

We construct a generic model of Majorana fermion dark matter (DM). Starting with two Z_2-odd Weyl spinor multiplets $\eta_{1,2} \sim (I, \mp Y)$ coupled to the standard model (SM) Higgs, eight additional Z_2-odd Weyl spinor multiplets with $(I \pm 1/2, \pm(Y \pm 1/2))$ are needed in general. It contains 13 parameters in total, five mass parameters and eight Yukawa couplings. The DM sector of the minimal extension of supersymmetric stand model (MSSM) is a special case of the model with $(I,Y) = (1/2, 1/2)$. Therefore, this model can be viewed as an natural extension of the MSSM case. We consider the cases of MSSM-like (A), MSSM-like (B), and an extended case. We study the constraints from the observation of dark matter in relic density, the direct detection of LUX and XENON100 experiments, and the indirect detection of Fermi-LAT data. From these constraints we can find the allowed range for each coupling strength. Without considering the outlier samples, we find that the DM mass for finding $\tilde{H}$, $\tilde{B}$-, $\tilde{W}$- and $\tilde{X}$-like DM particles should be greater than 445 GeV, 270 GeV, 1025 GeV, and 700 GeV respectively.

The European Physical Society Conference on High Energy Physics
22–29 July 2015
Vienna, Austria

*Speaker.

PoS(EPS-HEP2015)395

1. Introduction

Although the existence of dark matter (DM) has been well-established[1, 2, 3], we still know little about the nature of DM. One of the most prospective DM candidates is the so-called WIMPs (weakly interaction with massive particles)[4]. Except probing the WIMPs in the well-known models such as the minimal supersymmetric model (MSSM)[5, 6], using a model-independent model with the effective operators of dark matter coupled to standard model (SM) particles[7, 8] or constructing a simplified dark matter model that DM couples SM particles via a mediator[9, 10, 11, 12] are the usual ways to understand the DM properties. Due to the fact that the Dirac fermion DM gives an oversized spin-independent (SI) scattering off nuclei except for the special choice of DM quantum number[13], we provide another way by constructing a generic model of Majorana fermion DM without additional mediator.

2. Model Construction

With the standard model, we add two Z_2-odd 2-component Weyl spinors multiplets $\eta_{1,2} \sim (I, \mp Y)$ and consider all possible renormalizable interactions with $\eta_{1,2}$ coupled to the standard Higgs $\Phi \sim (1/2, 1/2)$. In other words, we consider the renomalizable terms with types like $\Phi \times \eta_{1,2} \times [new]$ and $\tilde{\Phi} \times \eta_{1,2} \times [new]$. We find that we need eight additional Weyl spinor multiplets $\eta_3, \eta_4, \cdots, \eta_{10}$ transforming as $(I \pm 1/2, \pm(Y \pm 1/2))$ under $SU(2) \times U(1)$ shown in Table1.

Multiplet	η_1	η_2	η_3	η_4	η_5	η_6	η_7	η_8	η_9	η_{10}
Isospin	I	I	I-1/2	I-1/2	I+1/2	I+1/2	I-1/2	I-1/2	I+1/2	I+1/2
Hypercharge	-Y	Y	-(Y-1/2)	(Y-1/2)	-(Y-1/2)	(Y-1/2)	-(Y+1/2)	(Y+1/2)	-(Y+1/2)	(Y+1/2)

Table 1: Model construction

The introducing of Z_2 symmetry assures the stability of DM. From the above particle content, the generic Lagrangian is given by

$$
\begin{aligned}
-\mathscr{L}_m = & \sum_{p=1}^{5} \mu_p \lambda^p_{ij} \eta^i_{2p} \eta^j_{2p-1} + \sum_{p=2}^{3} (g_{2p-1} \lambda^p_{ijk} \tilde{\phi}^i \eta^j_2 \eta^k_{2p-1} + g_{2p} \lambda^p_{ijk} \phi^i \eta^j_1 \eta^k_{2p}) \\
& + \sum_{p=4}^{5} (g_{2p-1} \lambda^p_{ijk} \phi^i \eta^j_2 \eta^k_{2p-1} + g_{2p} \lambda^p_{ijk} \tilde{\phi}^i \eta^j_1 \eta^k_{2p}) + h.c.. \qquad (2.1)
\end{aligned}
$$

In the above, λs are related to the Clebsch-Gordan coefficients and the superscript in η represents the third component of isospin. There are five mass parameters $\mu_{1\sim5}$ and eight Yukawa couplings $g_{3\sim10}$ in this model. The Majorana particles can access only when $Y = 1/2$, where the quantum numbers of $\eta_{3(5)}$ and $\eta_{4(6)}$ are identical, and hence I can only be half integral for having integer-charged particles. In parallel with MSSM, we only consider the model with $I = Y = 1/2$. In this case, η_3 is neutral singlet while η_7 and η_8 are singlets with charge ∓1. With the basis $\Psi^{0T}_i = (\eta_1^{1/2}, \eta_2^{-1/2}, \eta_3^0, \eta_5^0, \eta_9^1, \eta_{10}^{-1})$, the Lagrangian for neutral Z_2-odd fermion mass term can be extracted as

$$
\mathscr{L}^0_m = -\frac{1}{2} \Psi^{0T} Y \Psi^0 + h.c., \qquad (2.2)
$$

where the corresponding mass matrix Y takes the form

$$\begin{pmatrix} 0 & -\mu_1 & -\frac{g_4 v}{\sqrt{2}} & \frac{g_6 v}{\sqrt{2}} & 0 & g_{10} v \\ -\mu_1 & 0 & \frac{g_3 v}{\sqrt{2}} & \frac{-g_5 v}{\sqrt{2}} & g_9 v & 0 \\ -\frac{g_4 v}{\sqrt{2}} & \frac{g_3 v}{\sqrt{2}} & \mu_2 & 0 & 0 & 0 \\ \frac{g_6 v}{\sqrt{2}} & \frac{-g_5 v}{\sqrt{2}} & 0 & \mu_3 & 0 & 0 \\ 0 & g_9 v & 0 & 0 & 0 & \mu_5 \\ g_{10} v & 0 & 0 & 0 & \mu_5 & 0 \end{pmatrix}. \tag{2.3}$$

Comparing to MSSM[14], we see that the MSSM mass matrix of neutralinos is the upper left 4×4 matrix embedded in the 6×6 mass matrix of Eq. (2.3) with the following relations

$$\begin{aligned} \eta_1 = \tilde{H}_1, \eta_2 = \tilde{H}_2, \eta_3 = -i\lambda', \eta_5^{\pm,0} &= -i(\mp\lambda_\pm, \lambda_3), \\ g_3 v = \sqrt{2} m_Z \cos\beta \sin\theta_W, &\quad g_4 v = \sqrt{2} m_Z \sin\beta \sin\theta_W, \\ g_5 v = \sqrt{2} m_Z \cos\beta \cos\theta_W, &\quad g_6 v = \sqrt{2} m_Z \sin\beta \cos\theta_W, \\ \mu_4 = \mu_5 = 0, &\quad g_{7,8,9,10} = 0. \end{aligned} \tag{2.4}$$

3. Results

In parallel with MSSM[14], we analyze the model with $I = 1/2$ and $Y = 1/2$. For the MSSM-like case, the Majorana DM generated by $\eta_{1,2,3}$ and the triplet η_5. We will consider two subcases: (A) with the (grand unifie theory) GUT relation and $\tan\beta = 2$, (B) without the GUT relation and $\tan\beta = 2$. In the above, $\tan\beta = g_4/g_3 = g_6/g_5$ and the GUT relation means $\mu_2 = \frac{5}{3}\mu_3 \tan^2\theta_W$. Besides, we also consider the extended case with the maximal particle content. In each case, we survey the DM mass m_χ in the range of $(1, 2500)$ GeV by random sampling the mass couplings $\mu_i (i = 1\sim 5)$ in the range of (0,5000) GeV and the Yukawa coupling $g_i (i = 3\sim 10)$ in the range of (0,1) if these parameters are not set to zeros. In each case, we generate 10,000 random samples. For each sample, we numerically solve the freeze-out temperature parameter X_f and obtain the DM thermal relic density $\Omega_\chi h^2$ via the calculations of DM annihilation processes of ($\chi\bar{\chi} \to W^+W^-, ZZ, ZH, HH, q\bar{q}, l^-l^+$) to compare with the observed relic density $\Omega_\chi^{\mathrm{obs}} h^2 = 0.1198 \pm 0.0026$[15]. We calculate the normalized SI, SD (normalized to neutron and proton) scattering cross sections of Xe nuclei: σ^{SI}, σ_n^{SD} and σ_p^{SD} to compare with the results of direct search experiments of LUX[16], XENON100[17] collaborations. On the other hand, Fermi-LAT Collaboration[18] have presented six upper limits on the velocity averaged DM annihilation cross section $\langle\sigma(\chi\bar{\chi} \to W^+W^-, b\bar{b}, u\bar{u}, \tau^+\tau^-, \mu^+\mu^-, e^+e^-)v\rangle$ from a combined analysis of 15 dSphs so that we also calculate the velocity averaged cross section to compare with them. Hence we will use these ten constraints to find the allowed DM candidates.

For the direct search, we only show the scatter plot of σ_n^{SI} versus m_χ since σ_n^{SD} and σ_p^{SD} are linearly related to σ_n^{SI} and the LUX limit gives us the most stringent constraint among them. For the indirect search, we only show the plots of $\langle\sigma_{W^+W^-}v\rangle$ and $\langle\sigma_{b\bar{b}}v\rangle$ since it become less important for other DM annihilation channels. Before showing our results, we first define the higgsino-, bino-, wino-, nonMSSM-like particle if main ingredient ($> 60\%$) of a sample is in the state of (η_1 or η_2), η_3, η_5 and (η_9 or η_{10}) and denote by $\tilde{H}$-, $\tilde{B}$-, $\tilde{W}$- and $\tilde{X}$-like respectively; otherwise, we call it a mixed particle. In the subsequent descriptions, we will use 'red $\circ$', 'blue $\times$', 'green

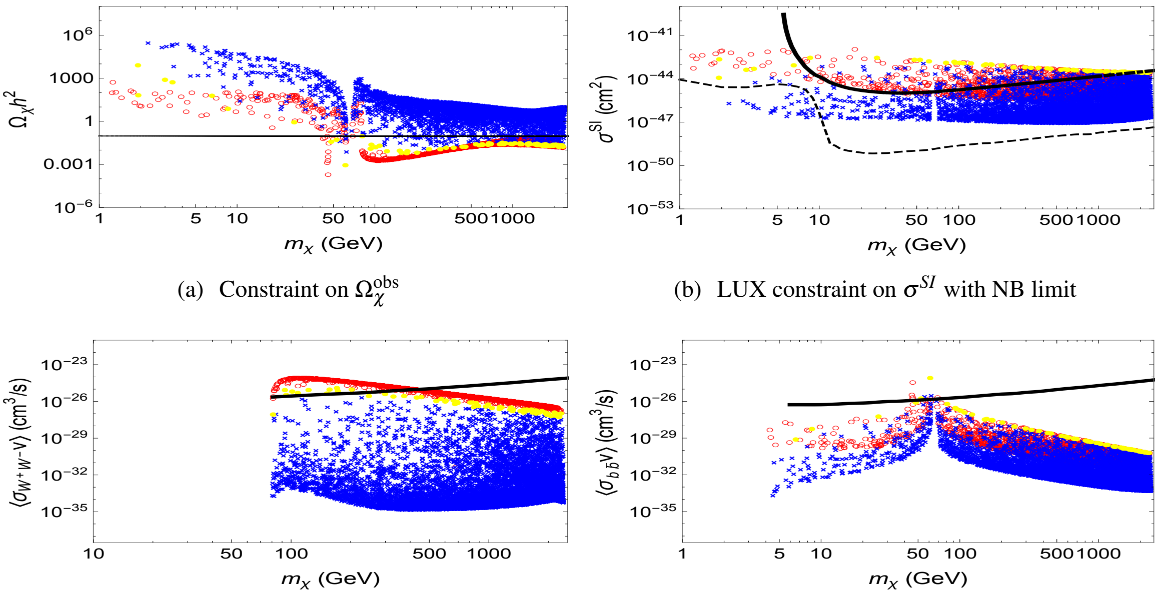

(a) Constraint on $\Omega_\chi^{\rm obs}$ (b) LUX constraint on σ^{SI} with NB limit

(c) Fermi-LAT constraint on $\chi^0\bar{\chi}^0 \to W^+W^-$ (d) Fermi-LAT constraint on $\chi^0\bar{\chi}^0 \to b\bar{b}$

Figure 1: Results for all samples with four constraints in the case of MSSM-like (A)
[○: higgsino-like, ×:bino-like, •: mixed]

△', 'magenta ■' and 'yellow •' denote the higgsino-, bino-, wino-, non MSSM-like and mixed particles respectively. We show our results in Fig. 1-3 with all samples. We emphasize on the interplay among these ten constraints using Fig. 1 in the case of MSSM-like (A), and then tell the differences among the cases. For MSSM-like (A) case, we show the scatter plot of $\Omega_\chi h^2$ versus m_χ in Fig. 1(a). The samples sitting above the observed horizontal line are ruled out. We see that most of $\tilde{B}$-like particles are ruled out, and $\tilde{H}$-like particles tend to have smaller values in relic density when $m_\chi > M_W$. It is the most stringent constraint since about 75% of samples are ruled out by this $\Omega_\chi^{\rm obs} h^2$ constraint. The (σ^{SI}, m_χ)-plot with LUX constraint are shown in Fig. 1(b). We find that mixed and $\tilde{H}$-like DM particles attend to have larger values while $\tilde{B}$-like DM particles attend to have smaller values in the DM scattering cross section off Xe nuclei. Most mixed particles are ruled out by the LUX constraint and part of mixed particles are ruled out by the Fermi-LAT constraint via W^+W^- channel. We see the samples sitting below the upper limit of the LUX SI-experiment[16] (solid curve) and above the line of neutrino background (dashed curve) are allowed so that about 91% of samples are saved. However, most $\tilde{B}$-like particles sitting in between have been ruled out by the $\Omega_\chi^{\rm obs} h^2$ constraint, and hence only 19% of samples are survived and 96% of survived samples are $\tilde{H}$-like. Hence the relic density and direct search constraints are complementary to each other.

The scatter plots of velocity averaged cross section of DM annihilation processes of $(\chi\bar{\chi} \to W^+W^-, b\bar{b}$ are shown in Fig. 1(c)-(d) respectively. The samples sitting above the Fermi-LAT constraints ruled out. We see that the $\tilde{B}$-like DM particles tend to have a smaller value of velocity averaged cross section while $\tilde{H}$-like and mixed DM particles tend to have a larger value of velocity averaged cross section, For W^+W^- channel, we see that part of $\tilde{H}$-like and mixed particles are ruled out by this constraint. Hence about 93% of samples are saved; however, most $\tilde{B}$-like and

PoS(EPS-HEP2015)395

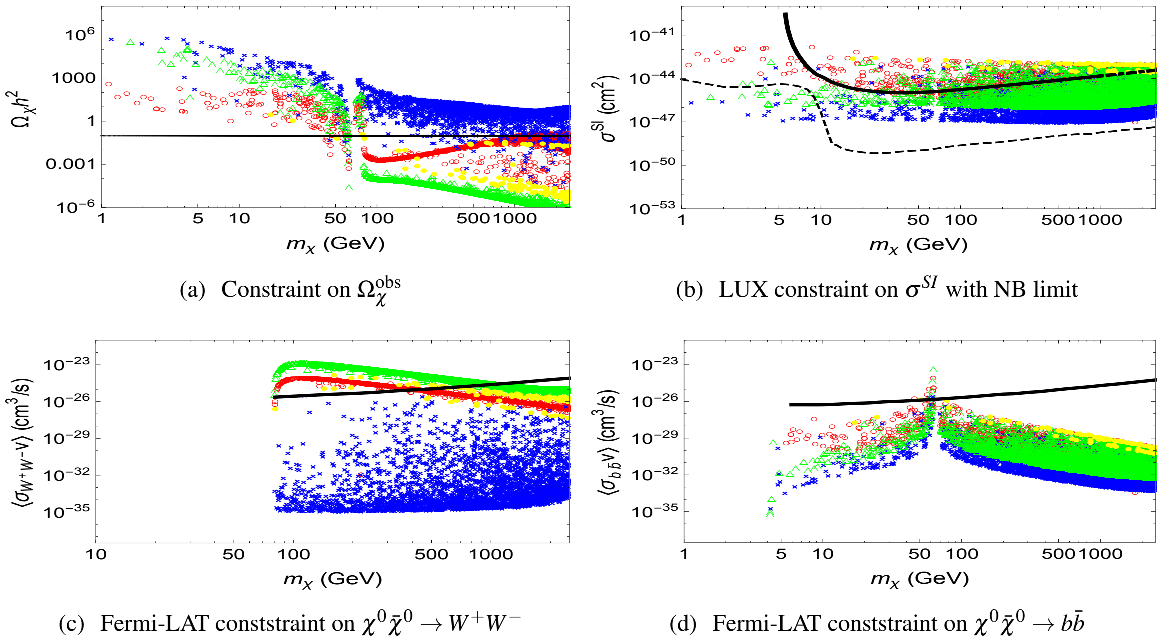

(a) Constraint on Ω_χ^{obs} (b) LUX constraint on σ^{SI} with NB limit

(c) Fermi-LAT conststraint on $\chi^0\bar{\chi}^0 \to W^+W^-$ (d) Fermi-LAT conststraint on $\chi^0\bar{\chi}^0 \to b\bar{b}$

Figure 2: Results for all samples with four constraints in the case of MSSM-like (B) [○: higgsino-like, ×: bino-like, △: wino-like, •: mixed]

sitting below the limit on ruled out by the relic density constraint and hence only about 18% of samples are still survived. For DM annihilation to $q\bar{q}$ or l^+l^- with final particle mass less than m_W, all have the same resonance shape as in Fig. 1(d). The peaks occur at $m_\chi = m_Z/2$, or $m_H/2$. For $b\bar{b}$ and $\tau^+\tau^-$ channels, only a few $\tilde{H}$-, $\tilde{B}$- and mixed particles are ruled out by this constraint and the constraint become less important when a final particle mass is less than m_τ. We see that the relic density is approximately proportional to the inverse of total cross section of DM annihilation to all possible channels. Hence the relic density is dominated by W^+W^- channel as $m_\chi > M_W$ and $b\bar{b}$ channel as $m_\chi < M_W$. These give the shape of relic density in Fig. 1(a).

Now we turn to see the differences among these three cases. First of all, we see the case of MSSM-like (A) with GUT relation. It is prohibited from generating the the $\tilde{W}$-like particles with GUT relation. Without GUT relation, plenty of $\tilde{W}$-like particles can be generated as in the case pf MSSM-like (B) and the extended cases. The non MSSM-like $\tilde{X}$ particles can only exist in the extended case. For the MSSM-like cases, we see that "without GUT relation" gives a wider spread in each scatter plot and most $\tilde{B}$-like particles are ruled out by the constraint of DM relic density. For the extended case, more $\tilde{B}$-like particles with lower values in DM relic density and less $\tilde{H}$-like particles with lower values in the DM scattering cross sections off nuclei are allowed. Although most $\tilde{B}$-like particles are ruled out by the constraint of DM relic density, most $\tilde{W}$-like particles with $m_\chi > m_W$ are not. The $\tilde{W}$-like particles are ruled out mainly by the Fermi-LAT constraint via W^+W^- channel and followed by the LUX constraint. Without GUT relations, the extended cases can have a wider spread in each scatter plot than the cases of MSSM-like (B) so that more $\tilde{B}$-like particles in extended case are allowed than those particles in the cases of MSSM-like (B). Finally, although there are only about 6% of the samples are non MSSM-like in the extended case, the $\tilde{X}$-

PoS(EPS-HEP2015)395

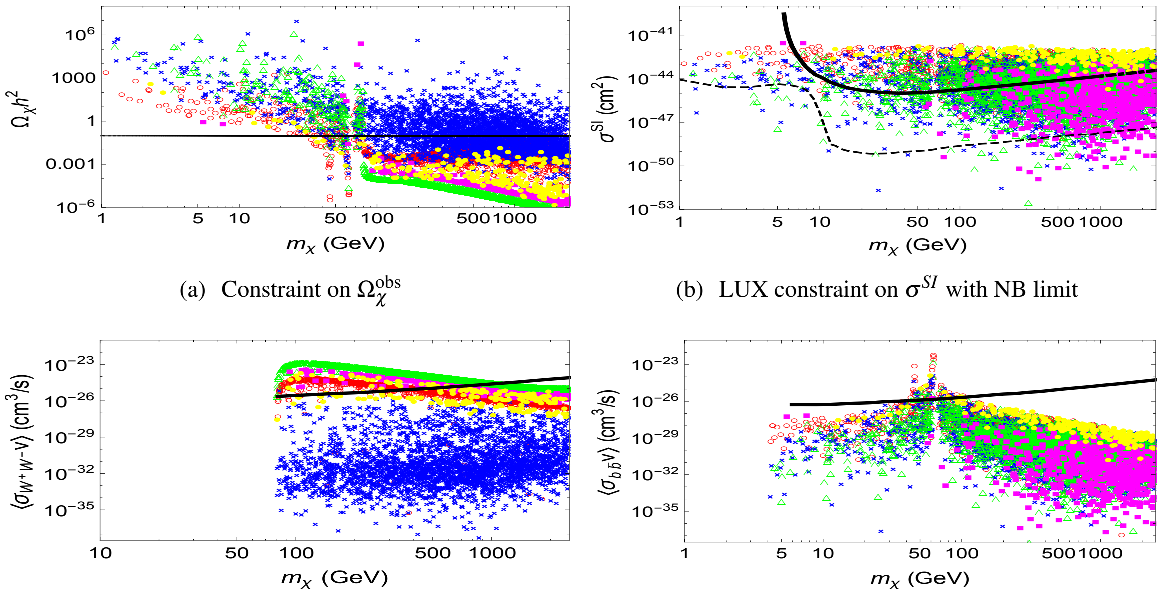

(a) Constraint on $\Omega_\chi^{\rm obs}$

(b) LUX constraint on σ^{SI} with NB limit

(c) Fermi-LAT constraint on $\chi^0\bar{\chi}^0 \to W^+W^-$

(d) Fermi-LAT constraint on $\chi^0\bar{\chi}^0 \to b\bar{b}$

Figure 3: Results for all samples with four constraints in the extended case
[○: higgsino-like, ×: bino-like, △: wino-like, ■: nonMSSM-like, ●: mixed]

like particle tend to have smaller values both in DM relic density and DM scattering cross section off the nucleon so that more than 50% of $\tilde{X}$-like particles are allowed for DM particles. We collect all allowed samples which satisfy all of constraints. Without considering the outlier samples, we find that the lower mass bound for finding $\tilde{H}$, $\tilde{B}$-, $\tilde{W}$- and $\tilde{X}$-like DM particles should be greater than 445 GeV, 270 GeV, 1025 GeV, and 700 GeV respectively.

4. Conclusions

We construct a generic model of Majorana fermion DM. The DM sector of MSSM is embedded in this model with $I = Y = 1/2$. The model does not contain the sfermions and the second Higgs as in the MSSM, but does contain more Z_2-odd fermion multiplets $\eta_{7,8,9,10}$. There are 5 mass parameters and 8 Yukawa couplings in this model. We collect all allowed DM candidates which satisfy the observed relic density, the lower bounds of LUX and XENON100 experiments and Fermi-LAT constraints. From the allowed DM candidates, we can find the allowed region for each coupling strength. Here we give the different lower mass bounds for different attributed particles so that it is detectable with the model especially in the direct detection of SI scattering cross section off nuclei and the indirect detection of DM annihilation to W^+W^- channel for DM searches in near future.

References

[1] V. C. Rubin and W. K. Ford, Jr.,“Rotation of the Andromeda Nebula from a Spectroscopic Survey of Emission Regions,” Astrophys. J. **159**, 379 (1970).

[2] S. Carroll, "Astrophysics: Dark matter is real," Nature Phys. **2**, 653 (2006).

[3] D. N. Spergel, *et al.*, [WMAP Collaboration], "First Year Wilkinson Microwave Anisotropy Probe (*WMAP*) Observations: Determination of Cosmological Parameters," Astrophys. J. **148**, 175 (2003) arXiv:0302309 [astro-ph.CO].

[4] J. R. Ellis *et al.*, "Supersymmetric Relics from the Big Bang," Nucl.Phys. B**238**, 453-476 (1984).

[5] G. Jungman, M. Kamionkowski and K. Griest, "Supersymmetric dark matter," Phys. Rep. **267** 195 (1996).

[6] A. Fowlie *et al.*, "Dark matter and collider signatures of the MSSM," Phys.Rev. D**88**, 055012 (2013), arXiv:1306.1567 [hep-ph].

[7] P. Agrawal *et al.*, "A Classification of Dark Matter Candidates with Primarily Spin-Dependent Interactions with Matter," arXiv:1003.1912 [hep-ph].

[8] J. M. Zheng, *et al.*, "Constraining the interaction strength between dark matter and visible matter: I. fermionic dark matter," Nucl.Phys.B**854**,350-374 (2012), arXiv:1012.2022 [hep-ph].

[9] R. E. Shrock and M. Suzuki, "Invisible Decays of Higgs Bosons," Phys. Lett. B**110**, 250 (1982).

[10] Y. Bai, V. Barger, L. L. Everett, and G. Shaughnessy, "2HDM Portal Dark Matter: LHC data and the Fermi-LAT 135 GeV Line," Phys. Rev. D**88**, 015008 (2013), arXiv:1212.5604.

[11] Y. Bai and J. Berger, "Fermion Portal Dark Matter," JHEP **11**, 171 (2013), arXiv:1308.0612 [hep-ph].

[12] E. M. Dolle and S. Su, "Dark Matter in the Left Right Twin Higgs Model," Phys. Rev. D**77**, 075013 (2008), arXiv:0712.1234 [hep-ph].

[13] C. K. Chua and R. C. Hsieh, "A Study of Dirac Fermionic Dark Matters," Phys. Rev. D **88**, 036011 (2013) arXiv:1305.7008 [hep-ph].

[14] H. E. Haber and G. L. Kand, "The Search for supersymmetry: Probing physics beyond the standard model," Phys. Rep. **117** 75 (1985).

[15] K.A. Olive *et al.* (Particle Data Group), Chin. Phys. C, **38**, 090001 (2014).

[16] D. Akerib *et al.* [LUX Collaboration], "First results from the LUX dark matter experiment at the Sanford Underground Research Facility," Phys. Rev. Lett. **113**, 091303 (2014) [arXiv:1310.8214 [astro-ph.CO]].

[17] E. Aprile *et al.* [XENON100 Collaboration], "Limits on spin-dependent WIMP-nucleon cross sections from 225 live days of XENON100 data," Phys. Rev. Lett. **111**, 021301 (2013) [arXiv:1301.6620 [astro-ph.CO]].

[18] M. Ackermann [Fermi-LATCollaboration], "Searching for Dark Matter Annihilation from Milky Way Dwarf Spheroidal Galaxies with Six Years of Fermi-LAT Data," [arXiv:1503.02641 [astro-ph.CO]].